

Chapter 2

An Introduction to X-Ray Fluorescence (XRF) Analysis in Archaeology

M. Steven Shackley

As I have discussed in the last chapter, our goal here is not to elucidate XRF for the entire scientific community – this has been done admirably by others – but to translate the physics, mechanics, and art of XRF for those in archaeology and geoarchaeology who use it as one of the many tools to explain the human past in twenty-first century archaeology. While not a simple exercise, it has utility not only for those like us, who have struggled (and enjoyed) the vagaries of XRF applications to archaeological problems, but for a greater archaeology. First, we trace the basic history of X-rays used in science and the development of XRF for geological and archaeological applications, and the role some major research institutions have played in the science. Following this is an explanation of XRF that, in concert with the glossary, illuminates the technology.

History of XRF in Archaeology

X-rays were first discovered by the German physicist Wilhelm K. Röntgen (1845–1923) for which he won the Nobel Prize in 1901 (Röntgen, 1898). While X-rays have been used for commercial elemental analysis since the 1950s, X-ray spectroscopy is much older than that, dating back to 1909 when Charles G. Barkla found a connection between X-rays radiating from a sample and the atomic weight of the sample. In 1913, Henry G. J. Moseley helped number the elements with the use of X-rays, by observing that the K line transitions in an X-ray spectrum moved the same amount each time the atomic number increased by one (Moseley, 1913/14). He is credited with the revision of the periodic tables, which were based on increasing atomic weight, to periodic tables based on atomic number. He later laid the foundation

M.S. Shackley (✉)

Department of Anthropology, University of California, 232 Kroeber Hall, Berkeley,
CA 94720-3710, USA

e-mail: shackley@berkeley.edu

for identifying elements in X-ray spectroscopy by establishing a relationship between frequency (energy) and the atomic number, a basis of X-ray spectrometry.

The potential of the technique was quickly realized, with half of the Nobel Prizes in physics awarded to developments in X-rays from 1914 to 1924. Originally, X-ray spectroscopy used electrons as an excitation source, but the requirements of high vacuum, electrically conducting specimens, and the problem of sample volatility posed major roadblocks. To overcome these problems, an X-ray source with a metal target was used to induce the fluorescent emission of secondary X-rays in the sample. Excitation of the sample by this method introduced some problems by lowering the efficiency of photon excitation and requiring instrumentation with complex detection components. Despite these disadvantages, the fluorescent emission of X-rays would provide the most widely used tool for the analyst using commercial instruments.

Why Non-Destructive X-Ray Fluorescence Spectrometry?

XRF hardware, the design of this instrumentation, and the decisions made in the selection of a particular instrument are discussed later. The overarching assumption in this volume is that XRF, particularly energy-dispersive X-ray fluorescence (EDXRF) spectrometry, solves many of our problems in geoarchaeology. Mike Glascock covers this in some detail in Chap. 8, in a comparison of EDXRF with NAA. Here, the real positive and negative points of XRF in archaeology are discussed.

What is Good About XRF?

The appeal of X-ray analysis of archaeological specimens lies in its remarkable combination of practical and economic advantages:

- **Non-destructive**
In the vast majority of cases, analysed samples are not destroyed or changed by exposure to X-rays. They can thus be saved for future reference or used for other types of testing that may be destructive, such as obsidian hydration analysis.
- **Minimal preparation**
Many samples can be examined with little or no pre-treatment, including almost all obsidian artifacts. Many of the alternative techniques require dissolution procedures that are both time-consuming and costly in terms of the acids or other reagents required. While it is best to wash any sediments off archaeological specimens it has been shown that if the dirt is minimal, and the artefact has not been subjected to heat so high as to melt some sediment matrix onto the sample, vigorous cleaning is not necessary (Shackley and Dillian, 2002). This is mainly due to the penetration of X-rays in the mid-Z X-ray region beyond the surface,

and while it does incorporate any contamination on the surface it is generally not an issue if some soil remains in the flake scars. The analysed volume is very large compared to any surface contamination. This is not the case with most metals, where patination and chemical weathering can radically change the composition at the surface and yield erroneous results (Hall, 1960).

- **Fast**
X-ray spectrometry enables chemical compositions to be determined in seconds. For an analysis of the elements Ti-Nb on the Berkeley Spectrace and Thermo desktop instruments, at 200 live seconds per sample it takes about 5–6 min per sample depending on mass.
- **Easy to use**
Modern instruments run under computer control, with effective software to handle measurement set-up and results calculation. Tasks that once required the constant attention of a trained analyst can now be handled by skilled students and are fully automated (cf. Rindby, 1989; Lachance and Claisse, 1994).
- **Cost-effective**
Without the more involved sample preparation necessary in most WXRf and all destructive analyses, the cost is significantly lowered per sample.

While this suggests that XRF will solve all our problems, it is not the all-knowing black box we would like it to be (see Bouey, 1991).

What Non-Destructive EDXRF Will Not Do

- **Sample size limits:** Samples >10 mm in smallest dimension and >2-mm thick are optimal for EDXRF analyses (see Davis et al., 1998; Lundblad et al., 2008; Chap. 3 here). Why is this important? Shackley (1990) and, more recently, Eerkens et al. (2007) noted that for hunter-gatherers in the North American West, high residential mobility often requires that stone sources, including obsidian, be conserved for long periods of time. As an example, an archaic hunter will attempt to rejuvenate a dart point rather than making a new one whenever possible as he or she moves through the landscape. The rejuvenation of that point creates debitage that is quite small, often smaller than 10 mm. With modern recovery techniques, these small debitage are recovered much more often than they were in the past, and to make a long story short, Eerkens et al. (2007) found that, indeed, these small obsidian flakes in Great Basin sites indicated not only a greater distance from the original tool raw material, but also a greater diversity of sources than would be visible in an analysis of the larger flakes with EDXRF. So, while EDXRF can analyse much of the stone material left in prehistory, it may not solve all problems of interest to twenty-first century archaeologists. To be fair, however, the procurement ranges that could be reconstructed were relatively accurate with samples above the 10-mm threshold in the Eerkens et al. (2007) study, and NAA, which is essentially a destructive technique (see Chap. 8), had to be used on the smaller flakes.

Recently, however, thanks to the newer digital EDXRF instrumentation and tube collimation, we have been able to reach down to sizes of 2 mm with the ThermoScientific Quant'X EDXRF at Berkeley (see also Hughes, 2010).

- Restricted elemental acquisition: As discussed below, non-destructive XRF is restricted generally to a subset of the mid-Z X-ray region, the best portion including Ti-Nb, contains excellent incompatible elements for volcanic rocks (Cann, 1983; Shackley, 2005). While some rare earth elements and those with low atomic numbers or with very low concentrations can be useful in discriminating sources, in most cases XRF cannot solve that problem. This is discussed in detail in Glascock's comparison between XRF and NAA in Chap. 8.
- XRF cannot characterize small components – XRF like NAA is a mass analysis – every component in the irradiated substance is included in the analysis. It is possible to collimate the incoming X-rays from the tube and/or into the detector to focus on small components such as various minerals, but environmental scanning electron microscopy (ESEM), electron microprobe, or laser ablated-inductively coupled plasma-mass spectrometry (LA-ICP-MS) is much better suited for this kind of analysis. However, the bulk analysis of volcanic rocks has been shown to be quite effective as we argue in this volume.

It is true that XRF will not solve all our problems in archaeological provenance studies; it is simply the best non-destructive analytical tool at our disposal at this time.

Commercial X-Ray Spectrometry

Early on three types of spectrometers were available to the analyst. From the 1950s to 1960s nearly all the X-ray spectrometers were wavelength dispersive spectrometers, such as those used initially at Berkeley, and by Shackley at Arizona State University (Jack and Carmichael, 1969; Hall, 1960; Hughes, 1984; Jack and Heizer, 1968; Shackley, 1988, 1990). In a wavelength dispersive spectrometer, a selected crystal separates the wavelengths of the fluorescence from the sample by diffraction, similar to grating spectrometers for visible light. The other X-ray spectrometer available at that time was the electron microprobe, which uses a focused electron beam to excite X-rays in a solid sample as small as 10^{-12} cm³. The first microprobe was built by R. Castaing in 1951 and became commercially available in 1958. By the early 1970s, energy dispersive spectrometers became available, which use Li-drifted silicon or germanium detectors. The advantage these instruments brought to the field was the ability to measure the entire spectrum simultaneously. With the help of computers, deconvolution methods can be performed to extract the net intensities of individual X-rays more on that later.

Early Berkeley XRF Studies

One of the earliest, if not the earliest application of XRF, particularly EDXRF, in archaeology was at Berkeley; it was based on the primary WXRF work of Edward Hall at Oxford (1960). In 1960, Hall reported using a wavelength XRF at Oxford on Imperial Roman coinage, noting the problems with patination on these coins. Hall's paper still serves as a model for the issues surrounding XRF analyses of archaeological material. However, as Shackley has noted elsewhere, the University of California, Berkeley has played a major role in the application of XRF to archaeological problems (Shackley, 2005).

While it might seem egocentric of the editor to favour Berkeley's role in XRF analyses in archaeology, it is true that the Departments of Earth and Planetary Sciences (formerly Geology and Geophysics) and Anthropology have continually utilized XRF and particularly EDXRF for archaeological applications since the late 1960s. In the 1970s and again from the 1990s into the twenty-first century, over 90% of the XRF applications were and are in archaeology and geoarchaeology at Berkeley. There are, of course, very real technological and paradigmatic reasons for this. Geological and petrological theory in this new century are increasingly demanding greater and greater precision in analyses, a precision that XRF cannot offer compared with NAA or ICP-MS (see Chap. 8). Due to exciting new concepts in the relationships between mantle and crustal geology, isotope chemistry has increasingly supplanted much elemental chemistry in geology (see Weisler and Woodhead, 1995 for an archaeological example). Indeed, it seems that while geologists are still "XRF users", archaeologists are the XRF cadre in science these days. So, as at Berkeley, XRF in many institutions has become the purview of geoarchaeological science. Many advances in analytical XRF are coming from archaeology and geoarchaeology. The computer industry, engineering, construction (concrete) and the aircraft industry are still heavy users. Still, archaeology is one of the major "buyers" at Thermo Scientific for the Niton portable XRF (PXRF) instruments, and the QuanX, now Quant'X desktop instruments as well as very many other manufacturer's instruments. Three of the four EDXRF instruments that were used for studies in this volume are ThermoScientific (then ThermoNoran) QuanX or Quant'X machines or the earlier Spectrace instruments (purchased by Thermo). These laboratories are, in part, daughter labs of the 1970s Spectrace 440 instrument at Berkeley, and the original DOS software which has now been re-written as the WinTrace™ Windows application. As discussed below, many Masters and Ph.D. studies in archaeology, as well as Shackley's 1990s work at Berkeley, began on this Spectrace 440 EDXRF instrument. The first experiments on size and surface constraints in obsidian artefact studies with EDXRF were performed on this instrument and they formed the basis for Lundblad et al.'s Chap. 4 (Davis et al., 1998; Hampel, 1984; Jackson and Hampel, 1992; Shackley and Hampel, 1992; Chap. 3). Lundblad et al.'s Chap. 4 is based on the digital ThermoScientific QuanX instrument that was mainly championed at the University of Hawaii-Hilo by Professor Peter Mills, a Berkeley Ph.D. in anthropology. This is not an attempt to support this particular EDXRF instrument, but to highlight the interconnectedness of EDXRF

in archaeology and the primary role that Berkeley has played in its dominance in geoarchaeology today.

In 1968, Robert Jack and Robert F. Heizer (Departments of Geology and Geophysics, and Anthropology, UC, Berkeley) published the first X-ray fluorescence (XRF) spectrometric analysis of archaeological obsidian in the New World. The next year (1969), Jack and Ian Carmichael (Department of Geology and Geophysics, UC, Berkeley, now the Department of Earth and Planetary Science – EPS) published “The Chemical ‘Fingerprinting’ of Acid Volcanic Rocks”. And while Cann and Renfrew (1964) had 4 years earlier published their NAA characterization of Mediterranean obsidian, Berkeley’s XRF analysis of obsidian artifacts for source provenance was the first in the New World, and the first of a multitude of XRF obsidian projects at Berkeley. For over 40 years now, Berkeley has remained a centre for obsidian studies using XRF spectrometry (Jack, 1971, 1976; Jack and Carmichael, 1969; Jack and Heizer, 1968; see also Asaro and Adan-Bayewitz, 2007; Giaque et al., 1993 for the XRF work up the hill at Lawrence Berkeley National Lab). Robert Jack analysed over 1,500 obsidian artifacts worldwide during this period with Jackson (1974), and then Richard Hughes (1983, 1984), who began to focus on California and Great Basin studies. The list of ceramic, obsidian, and other rock provenance studies since that time in which Berkeley XRF facilities were used by faculty, graduate students, undergraduate students and scholars from other universities would fill pages (see Hughes 1983, 1984; Jackson 1974, 1986; Shackley, 2005). Since 1990, the Geoarchaeological XRF Laboratory at UC, Berkeley, has analysed tens of thousands of artifacts, mostly obsidian and other volcanic rocks, supporting faculty, student, government and cultural resource management studies worldwide, and particularly from the North American Southwest (see Shackley, 2005). While the early studies were primarily focused on developing source standard databases for various regions of the world to permit the identification of stone tool raw material sources, more recent graduate student and senior scholar research that uses these facilities is now integrating obsidian provenance studies into current archaeological theory and method in western North America, South America, East Africa, Oceania and Mesoamerica (Dillian, 2002; Hull, 2002; Joyce et al., 2004; Kahn, 2005; Negash and Shackley, 2006; Negash et al., 2006; Shackley, 1991, 1992, 1995, 1998a, 1998b, 2005; Silliman, 2000; Weisler, 1993). As we discuss in this volume, while other techniques have been shown to exhibit more instrumental precision, XRF, particularly energy-dispersive XRF, has remained the leader in non-destructive studies of artifacts (see Davis et al., 1998; Hughes, 1983; Shackley, 1998c, 2005; cf. Speakman and Neff, 2005).

The Portable EDXRF Revolution

As mentioned in the previous chapter, PXRF instrumentation is beginning to transform archaeological science. Indeed, many disciplines that need rapid in-field or museum compositional analyses are looking at PXRF. In 2008, Potts and West

published the edited volume “Portable X-ray Fluorescence Spectrometry” in the Royal Society of Chemistry series. And while the vast majority of chapters are devoted to physical science applications, two are focused on archaeological and museum applications (Cesareo et al., 2008; Williams-Thorpe, 2008). Recently there have been a number of comparative studies between lab/desktop EDXRF and PXRF with varying results (Pessanha et al., 2009). Craig et al. (2007) analysed the same prehistoric Andean obsidian artifacts through a partial blind test using the Berkeley *QuanX* EDXRF and a PXRF at MURR at the University of Missouri with what the authors considered good agreement in the mid-Z X-ray region (see discussion of X-ray regions below; Craig et al., 2007). However, two issues arose with the above study: (1) While there was a general, statistically significant agreement between the studies overall, significant differences occurred between EDXRF and PXRF in certain mid-Z elements; and (2) the error rate was noticeably higher, giving larger dispersions about the mean in biplots with PXRF (Craig et al., 2007). This was explained in part by differing calibration routines. However, my experience with the Thermo/Niton PXRF at Berkeley indicates that the calibration routine is quite similar to the ThermoScientific calibration routine in the WinTrace™ software for the Quant’X desktop, although the software is completely different in the Niton (we use 11 standards for calibration in the Niton, and used 13 for the older *QuanX* in the Craig et al., 2007 study).

Recently Pessanha et al. (2009) directly compared the matrix effects between PXRF and laboratory WXRF and found that the behaviour between the instruments was similar, although the PXRF presented a “tremendously high background when compared to the stationary [WXRF] one . . . and some of the trace elements were almost not detected” (2009:497). This is a phenomenon we have found in the Berkeley NITON and the loaned Bruker instrument.

It is important for archaeologists to be aware that currently marketed PXRF instruments are not empirically calibrated out of the box, like desktop instruments (see calibration discussion below). Until quite recently, both off the shelf Bruker and Niton systems were calibrated through a fundamental parameters routine or not at all, which is fine for presence/absence analyses, but not adequate for the level of accuracy needed in most geoarchaeological studies. I realize how tempting it is for archaeologists to purchase a relatively inexpensive PXRF instrument that will, seemingly, solve all of their problems. I have had two former students purchase or borrow two different PXRF instruments; both were told that the “instruments are calibrated”, and the results were disastrous. Just like any desktop instrument, in order to establish reliability of results, you must create an empirical calibration, with appropriate conditions and using international standards. Otherwise, the results may be internally consistent, as seen in the Craig et al. (2007) study, but could be incomparable to other studies that are or are not empirically calibrated. The new PXRF industry is definitely based on a *caveat emptor* philosophy. There indeed, may be a PXRF revolution in geoarchaeology, but it requires the same instrument set-up procedures as desktop instruments. Indeed, few archaeologists currently using PXRF instrumentation even analyse a standard during each group of runs. It is impossible, then, to determine whether the results are accurate (see

Glascok's discussion in Chap. 8). Nazaroff and Shackley (2009) recently combined a sample size study for PXRF, similar to the one for EDXRF discussed in Chap. 3, as well as a comparison of the results of the analysis of the same source rocks for the Antelope Creek locality at Mule Creek, New Mexico between a Bruker PXRF, the Berkeley empirically calibrated NITON PXRF and the Berkeley Quant'X (Shackley, 2005). The results were presented at the 2009 Geological Society of America meetings in Portland, Oregon: we can see that there are errors in the Bruker by a factor of 2–3, although some of the incompatible elements are very close. The number of elements from the Bruker analysis that are close to the source standard data is not necessary and sufficient to assign to source, or certainly separate the various localities like the multiple events at Mule Creek (see Shackley, 2005; Nazaroff and Shackley, 2009). The Bruker PXRF was not empirically calibrated, although Bruker claims it was “calibrated”, but it appears that this was a fundamental parameter calibration.

The current vogue in PXRF in American archaeology seems to be (probably based on the instruction from Bruker and others), that all that is needed is to compare the count determined spectra between two or more obsidian artifacts and the analyst can discriminate whether they are from the same source after normalization – a decidedly qualitative and observer-based technique. There are at least two very crucial problems with this technique. First, it assumes that the analyst's judgement is correct, leaving one open to significant observer error. In this context, one must have at least a complete source database for comparison, just as in quantitative analyses. Second, and much more important, even with an adequate database of sources, I have seen at least three pairs of sources, quite distant from each other, that overlap exactly even after normalization, one misassignment by an industry representative touting this technique! The source pairs are: (1) Pachuca and La Joya in Mexico (see Glascok here); (2) Malad, Idaho and Cow Canyon, Arizona; and (3) Antelope Wells, New Mexico and Chihuahua and the newly located Los Sitios del Agua source in northern Sonora. These sources are hundreds, if not thousands, of kilometres apart, and I doubt that any archaeologist could confuse the two. Malad and Cow Canyon require a rather precise barium measurement to discriminate an element currently measured poorly with most portable instruments, which do not acquire much over 45 kV and thus make it difficult to determine that element.

In 2007, during Berkeley's Archaeological Petrology Field School in New Mexico, we analysed two very small (≤ 10 mm) pieces of obsidian debitage from the Mockingbird Gap Clovis Site near Socorro, New Mexico at or near the time of excavation (Huckell et al., 2007). Table 2.1 exhibits the analysis of these samples by the Berkeley empirically calibrated Niton in the field, and the two samples on the Berkeley ThermoSpectrace QuanX, the same instrument used in the Craig et al. (2007) study. Both studies, because the Mount Taylor (Grants Ridge) source is an unusual mixed-magma source with high Y (not available with the Niton as purchased) and Nb, could assign these small samples to that source in the field (see Shackley 1998a, 2005). Other regional sources such as Vulture or Superior with relatively low mid-Z numbers may not be as easily discriminated (Shackley, 1995,

Table 2.1 Elemental concentrations for the analysis of two approximately 10-mm diameter obsidian debitage from the Mockingbird Gap Clovis Site, southern New Mexico with the Spectrace QuanX EDXRF and the Thermo Niton PXRF

| Sample/ instrument | Mn | Fe | Zn | Rb | Sr | Y | Zr | Nb |
|---|----------|------------|----------|----------|-------|--------|---------|---------|
| 419 (QuanX) | 920 | 8311 | 156 | 519 | 7 | 69 | 103 | 181 |
| 419 (NITON- PXRF) | 987 | 7700 | 171 | 486 | 13 | nr | 106 | 158 |
| 293 (QuanX) | 856 | 7798 | 180 | 490 | 5 | 79 | 101 | 172 |
| 293 (NITON- PXRF) | 656 | 6029 | 170 | 436 | 7 | nr | 100 | nr |
| Mean Grants Ridge (<i>n</i> = 15); ± = SD | 849 ± 64 | 8302 ± 385 | 154 ± 12 | 570 ± 29 | 4 ± 1 | 76 ± 3 | 119 ± 4 | 198 ± 6 |

PXRFAll Niton measurements made with the Niton sample holder. Mean “Grants Ridge” data are from the analysis of source standards with the Spectrace QuanX at Berkeley (see Shackley, 1998a)

2005). Indeed, a closer inspection of the data suggests that the empirically calibrated Niton is not as sensitive in the analysis of some elements particularly Mn, but again still exhibited an analysis that would allow for assignment to source. This is remarkable given that desktop EDXRF instruments are only useful down to about 10-mm samples with volcanic rocks as discussed earlier (see Davis et al., 1998, and Chap. 3, here; and Lundblad et al., 2008). Sample size is certainly an issue in PXRF analysis of volcanic rocks as in desktop instruments, but there is yet to be a systematic study similar to the Davis et al. (1998), Lundblad et al. (2008), and Chap. 3 studies with PXRF instruments, except for the Nazaroff and Shackley (2009) study that has been criticized by the PXRF industry.

This volume is not dedicated to PXRF; the Potts and West (2008) edited volume does that quite well. Liritzis and Zacharias here do a remarkable job as a 2009 example offering a review of the recent literature, and derive similar conclusions to the Craig et al. (2007) study and Williams-Thorpe’s chapter in the Potts and West (2008) volume (see also Phillips and Speakman, 2009; and Pessanha et al., 2009). Like any emerging technology, PXRF will rapidly become more refined, and someday may replace most desktop systems. However, with the low-energy input, it may be a while before such a small “gun” captures all the elements between Na and U with the same instrumental precision as high-input desktop instruments (Shackley, 2010).

The Physics and Instrumental Technology of XRF

As noted in the first chapter, we endeavour to make the use of XRF in archaeology and geoarchaeology as transparent and understandable as possible for archaeologists. There are a number of texts and papers devoted to a more specialist discussion

of XRF, mainly for physicists, chemists, and engineers who are more interested in the theory and, less so, in the method of XRF, but not as one of the many tools used by archaeologists to explain the past (Bertin, 1978; Franzini et al., 1976; Giaque et al., 1993; Jenkins et al., 1981, 1999). More recently, many web sites have discussions of XRF both commercial and academic (see especially <http://www.learnxrf.com/>). The remainder of this chapter is devoted to a rather in-depth discussion of XRF for archaeologists, many of who do not, unfortunately, have an extensive background in the physical sciences, especially those in the United States (Goldberg, 2008; Killick, 2008). Taken with the chapters here and the glossary in the back of the volume, we hope that a better understanding of the “black box” that is XRF will be easily grasped. Most of the chapters also discuss XRF for their particular application, from basalt or obsidian analyses with EDXRF, WXRf and NAA to the vagaries of PXRF. Again, for those who would like more depth, I refer you to Jenkins (1999) second edition of *X-Ray Fluorescence Spectrometry*. Most of those terms that are in *italics* are also defined in the glossary.

Theory and Derivation of XRF

X-rays are a short wavelength (high energy-high frequency) form of electromagnetic radiation inhabiting the region between gamma rays and ultraviolet radiation. The XRF method depends on fundamental principles that are common to several other instrumental methods involving interactions between electron beams and X-rays with samples, including, X-ray spectroscopy (e.g. SEM – EDS), X-ray diffraction (XRD) and wavelength dispersive spectroscopy (microprobe WDS).

The analysis of major and trace elements in geological materials by XRF is made possible by the behaviour of atoms when they interact with radiation. When materials are excited with high-energy, short wavelength radiation (e.g. X-rays), they can become ionized. If the energy of the radiation is sufficient to dislodge a tightly-held inner shell electron, the atom becomes unstable and an outer shell electron replaces the missing inner electron. When this happens, energy is released because the inner shell electron is more strongly bound compared with an outer one (Fig. 2.1). The emitted radiation is of lower energy than the primary incident X-rays and is termed fluorescent radiation, often called *fluorescence* in the vernacular. Energy differences between electron shells are known and fixed, so the emitted radiation always has characteristic energy, and the resulting fluorescent X-rays can be used to detect the abundances of elements that are present in the sample.

The Spectrum and Spectral Lines – The Electron Configuration of the Elements

This process of displacement of an electron from its normal or ground state is called *excitation*. The atom can return to the non-excited state by various processes, one of

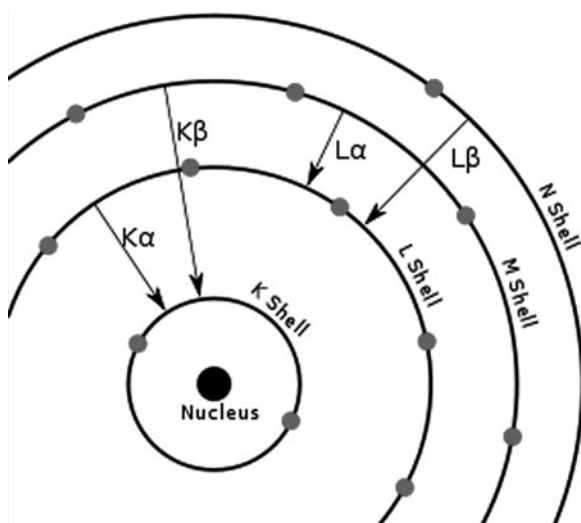


Fig. 2.1 Schematic view of orbital transitions due to X-ray fluorescence (see also Fig. 8.1 for an alternate view)

which is most important in XRF (Jenkins, 1999:55). When a substance is irradiated with high energy X-rays, electrons ejected from the atom produce an ion. The orbits or shells of an atom are called and read by the software as K through O lines (see Fig. 2.1). The K line transition is where the K electron moves out of the atom entirely and is replaced by an L line electron. Only the K and L lines are technically measurable with non-destructive XRF. X-rays of highest intensity from these transitions are called alpha transitions and are the transitions measured in all the XRF analyses in this volume (see Figs. 2.1–2.3). An L shell e-transition fills a vacancy in K shell and emits $K\alpha_1/K\alpha_2$ radiation. This is the most frequent transition, hence yielding the most intense and easily measured peak, the $K\alpha$ peak. These $K\alpha$ transitions are formed in doublets $K\alpha_1$ and $K\alpha_2$. $L\alpha$ lines sometimes measured for those high Z elements such as Ba, particularly in WXRF instruments, are the result of M orbit transitions to L orbits. In Chap. 3, Davis et al. discuss the use of the $L\alpha$ line in the analysis of Ba with the ^{241}Am gamma ray source in the retired Spectrace 440 EDXRF instrument at Berkeley. However, as also discussed in that chapter, most EDXRF labs today use very high energy (≈ 50 kV) to excite the Ba atoms in volcanic rocks and measure the $K\alpha$ peaks. While this does not yield the accuracy of using a gamma ray source, it avoids the issues of gamma radiation problems in storage and use, and the Ba elemental concentrations are generally accurate enough for most source assignments. Parenthetically, PXRF instruments are measuring Ba with much lower electron voltage. It remains to be seen what level of instrumental precision is offered in these instruments for the high atomic (Z) numbers.

Elemental Interference During XRF Analysis

While the measurement of fluorescent peaks in XRF seems straightforward, there are a number of interference issues that must be accounted for in all analyses. Many natural rocks consist of several different minerals of highly variable composition and structure. Even natural glasses that are amorphous with no crystalline structure are mixtures of a wide variety of chemical elements. This variable composition causes rocks to affect the behaviour of photons in highly complex ways. These effects on light translate directly to complexities in interpreting the fluorescence radiation that is detected in the XRF spectrometer. The complexities are collectively known as *matrix effects* which can be subdivided into overlap effects and mass absorption effects. The matrix effects on element i are the combination of mass absorption effects and overlap effects exerted on element i , by all coexisting elements j .

In Figs. 2.2 and 2.3, the spectra for the obsidian USGS standard RGM-1 prepared as a pressed powder pellet, the overlap between elements are readily observable. As an example, in Fig. 2.2, the mid-Zb analysis and ratio to the Compton scatter, Rb K β 1 overlaps the primary Nb K α 1 peak. These are called peak overlap or interference effects, and in early geoarchaeological studies using WXRF in particular, the software was not available to “strip” overlapping peaks from others by deconvolution

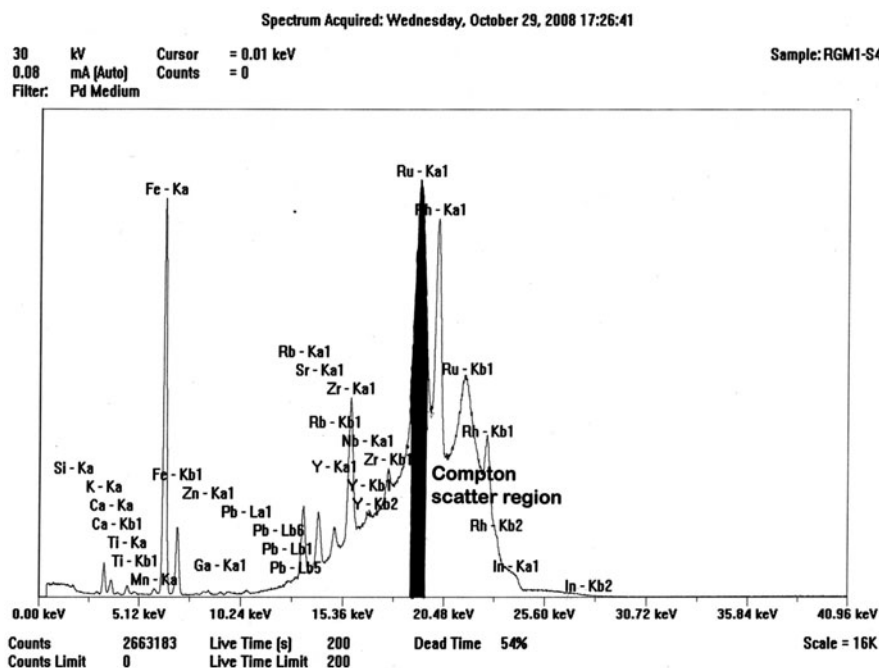


Fig. 2.2 Spectrum of the ThermoScientific Quant'X mid-Zb analysis of USGS RGM-1, showing the Compton scattered “hump” and that portion of the region under the Ru peak (*blackened*) used for peak ratioing

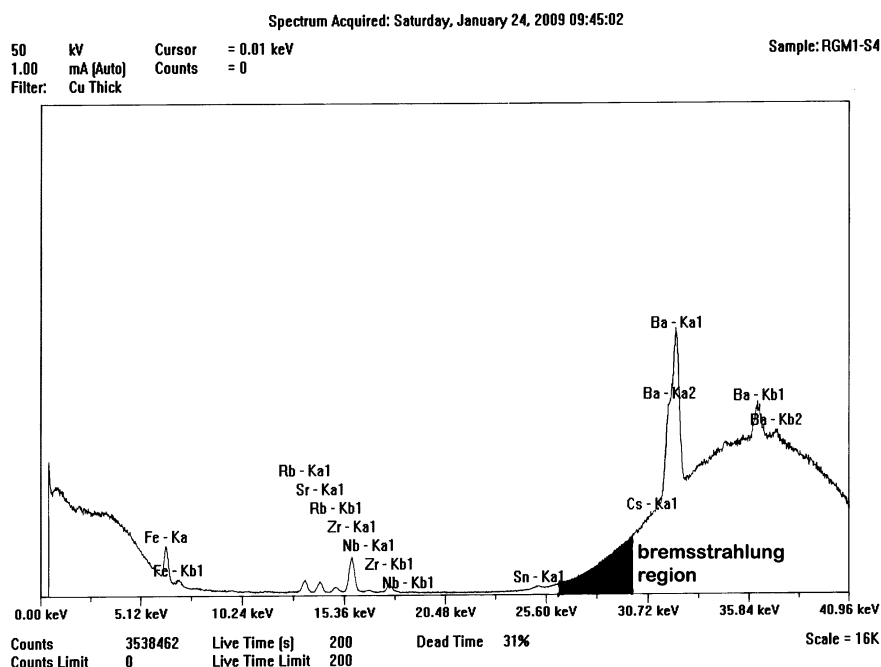


Fig. 2.3 Spectrum of the ThermoScientific Quant'X high-Za analysis of USGS RGM-1, showing the bremsstrahlung region and that portion of the region (*blackened*) used for peak ratioing

(Hughes, 1983, 1984; Ivanenko et al., 2003; Shackley, 1988, 1990). In this case, the peak heights were ratioed to others providing a semi-quantitative analysis. These semi-quantitative analyses were found to be problematic, because it is possible for two or more volcanic sources to have the same ratio of the selected elements, but different concentrations. In the North American Southwest, this is the case with the Antelope Wells (El Berrendo) obsidian source in southwestern New Mexico/northwestern Chihuahua and the recently discovered Los Sitios del Agua source in north-central Sonora, sources hundreds of kilometres apart (Martynec et al., 2010; Shackley, 1988, 1995, 2005). They are both *peralkaline* or mildly *peralkaline* glasses with very different elemental concentrations, but when plotted on the older ternary systems, they plot at the same point. Quantitative analyses (weight % and parts per million measurements, PPM) effectively solve this problem.

Not apparent in the spectra are *mass absorption effects*. Mass absorption effects result from fluorescence radiation being absorbed by coexisting elements (causing reduced intensity), or enhancement of fluorescence radiation due to secondary radiation from itself or coexisting elements (causing increased intensity). In many cases the effects can be effectively eliminated by proper sample preparation in pressed powder or fused disk samples, but corrections can be made in any case even when analysing samples non-destructively.

Table 2.2 X-ray fluorescence concentrations for selected trace elements of RGM-1 pressed powder pellet ($n = 35$ runs), and whole rock flake from original USGS Glass Mountain boulder ($n = 12$)

| SAMPLE | Ti | Mn | Fe | Rb | Sr | Y | Zr | Nb | Ba | Pb | Th |
|--|------------|----------|-------------|---------|----------|-----------------|----------|-----------|----------|----------|----------|
| RGM-1 (Govindaraju, 1994 recommended) | 1600 | 279 | 12998 | 149 | 108 | 25 | 219 | 8.9 | 807 | 24 | 15.1 |
| RGM-1 (USGS recommended) ^a | 1619 ± 120 | 279 ± 50 | 13010 ± 210 | 150 ± 8 | 110 ± 10 | 25 ^b | 220 ± 20 | 8.9 ± 0.6 | 810 ± 46 | 24 ± 3 | 15 ± 1.3 |
| RGM-1, pressed powder (this study, $n = 35$) | 1563 ± 60 | 302 ± 14 | 13116 ± 308 | 151 ± 3 | 106 ± 3 | 25 ± 2 | 219 ± 5 | 9 ± 2 | 869 ± 61 | 26 ± 2 | 16 ± 3 |
| RGM-1, flake from original USGS boulder ($n = 12$) | 1568 ± 44 | 311 ± 11 | 13306 ± 33 | 153 ± 2 | 113 ± 2 | 25 ± 1.5 | 230 ± 4 | 9 ± 2 | 842 ± 14 | 23 ± 1.5 | 15 ± 3.4 |

Plus or minus values represent first standard deviation computations for the group of measurements. All values are in parts per million (ppm) as reported in Govindaraju (1994), USGS, and this study. RGM-1 is a U.S. Geological Survey obsidian standard obtained from Glass Mountain, Medicine Lake Highlands Volcanic Field, northern California. All samples analysed on the ThermoScientific Quant'X EDXRF spectrometer at Berkeley

^aTi, Mn, Fe calculated to ppm from weight % from USGS data

^bInformation value

Today, matrix effects particularly mass absorption and overlap effects are eliminated by stripping routines that calculate the intensity of each element of interest and “strip” them from overlapping elements. This is a tremendous advancement in the software routines in XRF and invisible to the analyst (see Ivanenko et al., 2003; Lachance and Claisse, 1994; McCarthy and Schamber, 1981; Schamber, 1977).

Issues of Practical Matrix Effects

Practical matrix effects here are the practical issues of analysing two different matrices, such as pressed powder standards and analysed whole rock. We have worried about this for a number of years. Most of us using EDXRF instruments use pressed powder pellets of international standards for calibration and checking various analytical runs. The question, posed by some, is whether setting up calibration routines with pressed powder pellets for the analysis of whole rock samples is skewing our results (Mike Glascock, personal communication 2009). One of the more common standards used is RGM-1, a U.S. Geological Survey obsidian standard from the Glass Mountain obsidian flow of the Medicine Lake Highlands of northern California. A 200 kg single block of obsidian was collected by USGS and powdered. It is sold, or was sold (there is a newer RGM-2) to anyone desiring the standard. I was able to procure a whole rock flake of RGM-1 from the original boulder from USGS, and using our calibration routine based on pressed powder pellet standards (see Appendix), derived very similar results from the flakes as the powdered standards (Table 2.2). We had also tested this years ago as reported here in Chap. 3. I think this is a non-issue, at least for obsidian.

Evaluating Spectra: Compton, Bremsstrahlung and Other Spectral Issues

Evaluating merely the elemental spectra is only part of the work performed by the XRF analyst and the software available. The influence of the background radiated, often called “scatter” in the XRF vernacular, is important to understand, and is useful in determining the quantitative composition of a sample through “ratioing”.

Backscatter

Some of the X-rays strike the sample itself (i.e. an obsidian artefact) and are scattered or reflected directly into the detector. For instrumental XRF, this is one form of scatter that is stripped from the analysis even though the quantity of backscatter is mass dependent (Jenkins, 1999, 24–25).

Rayleigh Scatter

The Rayleigh scatter, also called elastic or coherent scatter, occurs as a result of a portion of the X-rays from the tube bouncing off the atoms without producing fluorescence, but it occurs as a source peak in the analysis. In essence, the high-energy X-rays directed at the atoms in the sample are partially redirected into the detector from the atoms directly. In Figs. 2.2 and 2.3 they are part of the elemental peaks seen in the spectrum but are not measured in the analysis, just as with backscattering energy.

Escape Peaks

In a gamma or X-ray spectrum, the peak due to the photoelectric effect in the detector *escapes* from the sensitive part of the detector. In XRF systems with Si(Li) detectors (as in most systems discussed in this volume), as X-rays strike the sample and promote elemental fluorescence, some Si fluorescence at the surface of the detector escapes, but it is not collected by the detector. The result is a peak that

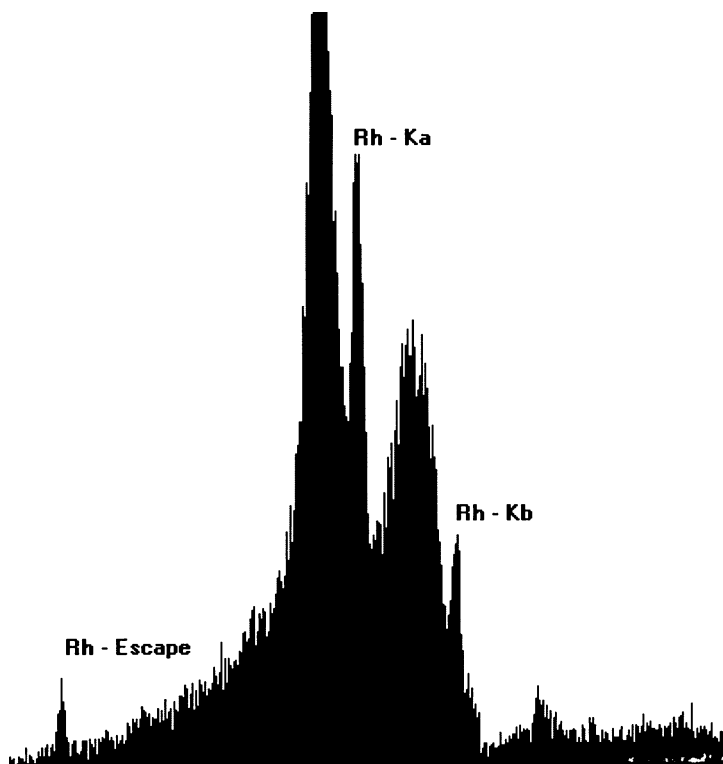


Fig. 2.4 A Compton scatter showing the Rh escape peak at 1.74 keV

appears in the spectrum, at: element keV – Si keV (1.74 keV; Fig. 2.4). In most archaeological applications, these escape peaks have virtually no relevance, but for quantitative geological applications, they are worthy of notice and calculation (Buras et al., 1974). Again, modern software virtually eliminates these peaks as an issue.

The Compton Scatter

An important portion of the spectra in the generation of quantitative elemental analyses in non-destructive XRF is the Compton scattered peak (Figs. 2.2 and 2.3). Also called incoherent or inelastic scattering that occurs when an X-ray photon collides with a loosely bound outer electron. The electron recoils under the impact, removing a small portion of the energy of the primary photon, which is then deflected with the corresponding loss of energy, or in WXRf increase of wavelength. There is a relatively simple relationship between the incident λ_o and incoherently (Compton) scattered wavelength λ_c :

$$\lambda_c - \lambda_o = 0.0242(1 - \cos\psi). \quad (2.1)$$

ψ is the angle over which the X-ray beam is scattered which in our spectrometers is equal to 90° . Since the cosine of 90° is 0, there is generally a fixed wavelength difference between the coherently (elemental in our case) and incoherently scattered lines equal to about 0.024 Å. As noted by Jenkins: “This constant difference gives a very practical means of predicting the angular position of an incoherently scattered line. Also the incoherently scattered line is much broader than a coherently scattered (or diffracted) line because the scattering angle is not a single value, but a range of values due to the divergence of the primary beam” (1999:12). This is crucial in both non-destructive EDXRF and WXRf applications where the artifacts have varying sizes and surface configurations. In tube driven XRF instruments, the Compton scattered peak or background is produced by the target (Rh targets in this volume) and produces those large Rh peaks, a portion of which is used for ratioing to the elemental peaks (Fig. 2.2). So, by ratioing to this Compton scatter, which is in essence a direct reflection of the mass of an object, a 10-mm piece of obsidian biface thinning debitage produced from the Sierra de Pachuca source in Hidalgo, Mexico, will have, through a non-destructive EDXRF analysis, the same composition as the much larger biface from which the flake was struck. Without the knowledge and application of the Compton scatter, we could not analyse archaeological material non-destructively.

The Bremsstrahlung Region

Bremsstrahlung (or continuum or continuous) radiation is the German for “breaking radiation”, noise that appears in the spectra due to deceleration of electrons as they

strike the anode of the X-ray tube. This is also frequently called the *background*. For the heavy incompatible elements such as Ba which are important for discriminating volcanic rock sources, bremsstrahlung scattering does appear at the heavy end of the spectrum. The bremsstrahlung radiation is produced by the tungsten (W) anode in the X-ray tube and (conveniently) provides a region for ratioing for the heavier elements as shown in Fig. 2.3. In the EDXRF case or in WXRf where ratioing is used for non-destructive analyses, a region must be chosen that does not contain any element of interest (see Davis, 1994; Chap. 3 here). So a region on the bremsstrahlung scatter is chosen for comparison and more specifically the region between Sn $K\alpha_1$ and Cs $K\alpha_1$ is used at Berkeley for ratioing for Ba analysis (see Fig. 2.3).

The Influence of “Background”

The term “background” used in the XRF vernacular is the bremsstrahlung radiation as discussed above. Since scatter increases with a decrease in the atomic number of the “scatterer”, backgrounds are much higher for low average atomic number specimens (or an analysts attempt to analyse elements of lower atomic number) than the background for higher atomic numbers. As an approximation, the background in XRF varies as $1/Z^2$. In essence, this is why Rh target EDXRF instruments and XRF in general are unable to reliably analyse below about $Z = 11$ (Na). The background in the low atomic number elements is relatively too high for XRF to deal with the counting errors vs. background. With an EDXRF Ag target instrument it is possible to get down to $Z = 9$ (F), but not easily. The term “mid- Z ” elements in XRF vernacular relate to those elements from about $Z = 19$ to $Z = 41$, and because the background effect is relatively inconsequential, those elements are analysed readily with predictable error.

In sum, the various spectra in the generation of X-rays have various uses in archaeological XRF analysis. X-ray tubes with tungsten anodes and rhodium or silver targets produce continuous radiation (W anode) and incoherent scattering (Ag or Rh targets) that have great utility in concert with modern software and precision detectors in providing good instrumental precision and analytical accuracy solving some of our more interesting and important problems in archaeology today.

XRF Hardware and Software

The foregoing discussion of XRF theory and method is only part of the story. Those of us involved in the XRF analysis of archaeological materials make hardware decisions for any number of reasons: (1) budgetary limitations obviously; (2) the history of certain hardware at our institutions or those where we learned XRF; (3) the types of materials analysed; (4) and institutional agreements that require purchasing from only certain suppliers.

In this section, the differences between EDXRF and WXRf, the important components of these instruments, and useful issues of instrument acquisition, calibration and the derivation of the results that we send to archaeologists are discussed.

Acquisition Condition Selection

Choosing optimal acquisition conditions for XRF analysis is a complex and critical part of the work, and to a certain extent part of the “art” of XRF spectrometry. Selecting the proper acquisition conditions can mean the difference between measuring an element at PPM levels, or not seeing it at all. There are two fundamental principles that must be met to achieve optimal analysis conditions.

There must be a significant source peak above *absorption edge* energy (the upper limit of the K or L radiation) of the element of interest. This may be either the K or L line depending on which one is appropriate as discussed above. The closer the source energy is to the absorption edge, the higher the intensity and sensitivity (counts per s/ppm) will be for the element of interest.

The other fundamental principle is that the background X-rays within the region of the elements of interest should be reduced as much as is practical. The difficulty is that these two principles work in opposition to each other, as the best sensitivity is often achieved when the background is highest, and the background is lowest when the sensitivity is poor – the weakness of XRF analysis. Added to this is the fact that the best theoretical detection limits are achieved when the sensitivity is highest, while the net count rate extraction, matrix corrections and long-term analytical stability are best when the background is lowest. Optimal analytical performance is achieved by finding the best compromise between these two principles, given the instrument hardware. In modern instruments, these issues are partly corrected by very real increases in the sensitivity of modern detectors and a shift from analogue to digital connections between the instrument and the computer and software.

Elements of Interest

The first step to setting up a XRF analysis is determining the elements of interest. If a sample or rock type has never been analysed for every conceivable element, the odds are high that it contains something that we might not expect. Some samples come into a laboratory as complete unknowns, such as obsidian artifacts from a region unfamiliar to analysts in the lab. For example, many of the rhyolite centres that produced obsidian in the Rift Valley in East Africa contain relatively high concentrations of Zn, much higher than obsidian in the rest of the world (Negash and Shackley, 2006; Negash et al., 2006). Zinc becomes one of the best discriminating elements in the region, particularly those sources in Ethiopia and to a certain extent the Near East, but has little utility in other regions.

If a sample is not well characterized, it is a good idea to perform a qualitative examination of the material using three or more acquisition conditions, designed to cover high, medium, and low energy ranges. Qualitative acquisition conditions will be covered below. Alternatively, a multivariate statistical analysis such as principal components analysis can isolate those elements of interest that are best discriminators in the region (see Glascock et al., 1998).

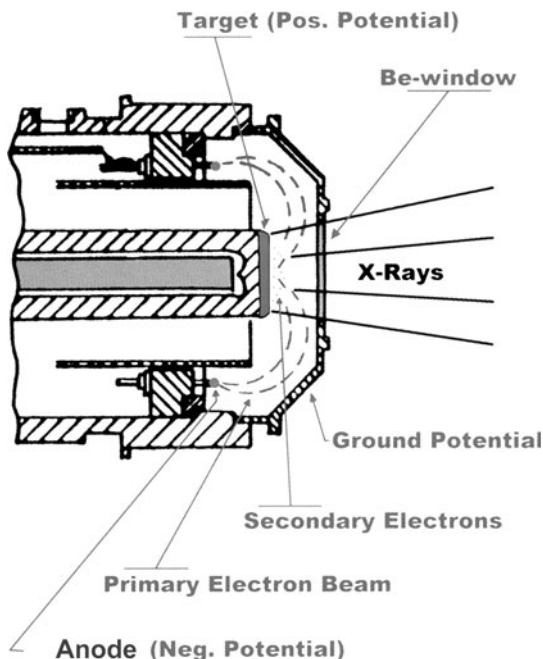
Source Selection – Isotopes

Isotopes are the simplest source to configure. Select a source that emits X-rays that are closest to and immediately above the absorption edge energy for the element of interest. To avoid problems with high background, the element of interest peak should be at least 2–3 times the *FWHM* (full width – half maximum of the peak) detector resolution away from the source peak. Davis et al. in Chap. 3 discusses the use of the ^{241}Am source at Berkeley in the 1990s for acquisition of barium that can be problematic with X-ray tube analyses as discussed above. *FWHM* is an expression of the extent of a function, given by the difference between the two extreme values of the independent variable (this would be the elements of interest) at which the dependent variable is equal to half of its maximum value (see X-ray filters below). In EDXRF this is also called resolution, calculated as the distance in electron volt between left and right sides of the peak at half of its maximum height, or more simply the peak width at half its height.

Source Selection – X-ray Tubes

X-ray tube selection is often done by the manufacturer without much input from the customer, but there are some selection rules that are useful. X-ray tubes emit a broad bremsstrahlung spectrum from 0 to X KeV, where X is the accelerating voltage of electrons that strike the metal target in the X-ray tube. The peak intensity in the bremsstrahlung spectrum is at roughly half the maximum energy. The X-ray tube also emits line energies that are characteristic of the target element, so target selection is usually based on selecting a target that will provide optimal excitation for the most important elements of interest. Alternatively, the selection is based on having a line energy that does not increase the background in the region of any important element. Since the amount of X-ray flux is proportional to the atomic number of the target element, anodes such as W are also selected on the basis of having the highest total flux. Targets can be any of several high-melting point metals. Common target choices include Sc, Ti, Cr, Fe, Co, Ni, Cu, Y, Zr, Mo, Rh, Pd, Ag, W, and Pt. Rhodium is the most common among the ones used in the EDXRF discussions in this volume, but as discussed above, Ag targets can aid in the acquisition of the lighter elements and can be constructed as easily as tubes with

Fig. 2.5 Schematic of a portion of a typical end-window X-ray tube



Rh targets (Richard Hughes, personal communication, February 2009; Franzini et al., 1976).

Multiple target tubes are often used in WXRf instruments, and they allow the operator to select the target on a per element basis, using the rule that the target with line energy immediately above the absorption edge is the one selected, providing it is at least 2–3 times the FWHM detector resolution away from the element line. If there is no target available with an emission line above the element of interest, the analyst or the software selects the highest atomic number target available to maximize the total X-ray flux from the tube.

Most modern EDXRF tubes are composed of a tungsten anode and an Rh or Ag target, and they are all end window tubes, such as the ThermoScientific products. Modern WXRf systems employ a variety of different tube configurations, and as mentioned below, multiple target and collimation configurations (Fig. 2.5)

X-ray Tube Filters

Filters are frequently placed in the X-ray path between X-ray tube and sample in order to modify the shape of the source spectrum. Filters can be made of any element that can be formed into a stable solid or film. They are usually metal or plastic although plastic filters deteriorate under prolonged bombardment by X-rays.

The key to the function of filters is the filter element's absorption edge energy. The filter readily absorbs source X-rays immediately above the absorption edge while those below the absorption edge are transmitted. Very high-energy X-rays are also transmitted. This produces a low background valley immediately above the filter's absorption edge that is crucial for analysing elements in the energy range beginning 2 FWHM detector resolution widths above the absorption edge. In the Thermo-Scientific EDXRF spectrometers, seven filters are used for analysis of elements between $Z = 11$ – 92 . As an example, for $Z = 37$ – 42 (Rb–Mo) a 0.06-mm Pd filter is optimal (called by Thermo the “Mid Zc” region). Palladium ($Z = 46$) is 3Z past Mo in the periodic table and over 2 FWHM past Mo. However, with proper calibration it is possible to get relatively accurate numbers for Ti–Nb, plus Pb and Th with the medium Pd filter with obsidian – a very homogeneous substance (see Shackley, 2005: Appendix). For the analysis of Ba, a 0.559 thick Cu filter is used. This is well beyond the FWHM, because the tube is operated at such a high energy, typically 50 kV and 0.5–2 mA.

Filters also fluoresce their own characteristic line energies, which combine with the bremsstrahlung that is transmitted by the filter to a region that resembles a right triangle (see Fig. 2.3). This secondary filter fluorescence peak can be used as a source peak for elements that are about 3 atomic numbers or more less than the filter element, as discussed above.

Another type of filter is a neutral absorbing filter such as aluminium or cellulose. These filters are intended to filter lower energy source X-rays in order to reduce the background in the region of the element of interest. A thin neutral density filter may be useful for measuring elements like S, or P with a Rh, Pd, or Ag target X-ray tube, while thicker Al filters can eliminate these target peaks entirely creating a source that is good for analysing X-rays ($K\alpha$ lines) between 2 and 10 keV (P–Ge elements). In the Thermo instruments, no filter is used for the very lowest end of the spectrum ($Z = 11$ – 16 ; Na–S). In this case, the energy is so low that any filter would reduce the very low fluorescence to near zero even in vacuum. In advanced PXRF instruments, a number of filters will be combined (i.e. aluminium, palladium) to enable a broad range of elemental acquisition. To my knowledge, this has not been tested experimentally, or at least reported.

Voltage Settings (kV)

Once the type of acquisition is determined, choosing the optimal X-ray tube voltage is the next step. Because of the broad energy distribution created by the X-ray generation process of an X-ray tube, the optimal high voltage is usually 1.5–2 times the absorption edge energy of the highest energy element in the acquisition. This element may be an element of interest but is more commonly the X-ray tube target, secondary target (not discussed here) or filter material. It may also be the K absorption edge $K\alpha$, $K\beta$, or the L absorption edge depending on which lines are being excited for analysis. If optimal deadtime (periods at which counts are not

taken because the detector is busy with earlier detected X-rays) or count rates cannot be achieved at the $1.5\times$ value due to current limitations of the tube or high voltage power (usually near 50%), then the high voltage should be increased until they are close to that level. In modern systems discussed here, the power setting (kV and mA) is generally set by the software, particularly for milliamperage (mA), the “push” or current of the voltage.

X-Ray Tube Target Excitation

If a characteristic target line is used to excite some elements, then the analyst selects a voltage $1.5\text{--}2\times$ its absorption edge. For example, in the Thermo instruments, if Rh K-lines are used as the excitation source and its $K\alpha\beta$ energy is 23.224 keV, then voltage is set in the 35–45 keV range. In the Thermo instruments, this is usually at the lower end (i.e. about 35 keV) for the mid-Zc region, in part because the digital pulse processors are much more efficient now.

When the bremsstrahlung continuum acts as the exciting radiation, then the high voltage should be $1.5\text{--}2\times$ the highest energy element of interest excited in that analysis condition. For example if we are measuring the Ba $K\alpha$ line with its 37.410 keV absorption edge, then 56 kV potential is recommended, but since the Rh target maximum is 50 kV, that is used. This is one reason that tube acquired Ba measurements are subject to such varying intensities, as found in the comparison with the use of the Am source (see Chap. 3). By using the thick Cu filter, some of this problem can be eliminated such that the error rates in the analysis of Ba are diminished.

Current (mA)

There is one simple rule for setting the current; measure the count rates or deadtime at the lowest current setting, usually 1 or 10 mA. The X-ray flux from the tube increases in direct proportion to the current so it is simple to extrapolate the needed current. The detector response is not quite linear, so an estimate of the current is needed to reach the instrument manufacturers specified optimal counts, and adjust the current upward. The reason this is done is that detectors do not respond well to excessive count rates, and if the maximum count rate has been unknowingly exceeded, the instrument will fail to make a proper measurement: essentially, when deadtimes get too high, peak resolution degrades. This is partly detected by the deadtime and in the Thermo WinTrace[™] software, it is noted in red on the monitor when it reaches a very high or very low point. Optimally, deadtime should be around 50%. By changing the current, the deadtime can be optimized.

In general, a higher current is required when operating at low voltages (less than 10 keV). In some cases, an instrument may have too high a count rate at the minimum current. In such case, the high voltage must be reduced or a different

filter or collimator selected. Most modern EDXRF instruments can set the optimal current for a given voltage that is sufficient for most applications. It is still a good idea to experiment with varying tube conditions, particularly if the range of elements of interest is outside that recommended by the manufacturer.

Tube Collimators

Collimators are another option in XRF instruments. In EDXRF systems, they usually have a single hole in the middle and can vary in size from 25 μm to several millimetres. Collimators are usually selected when small spot sizes are needed either because the sample is small or a specific point of interest on a sample is small. As mentioned above collimators are also used to reduce the X-ray intensity in some cases when sample size may be large and deadtime is too high, such as large obsidian or basalt bifaces or other large tools (see Lundblad et al., 2008; and Chap. 4). The collimator used on the Berkeley Quant'X is 8.8 mm in diameter and creates a 28 mm circular irradiated area on the samples. For most analyses, this is fine, but when the sample is very small, it is necessary to use a smaller collimator, 3.5 mm in this case. I have not found it to require a different calibration. It is important to remember that while *infinite thickness* (discussed in Chap. 3) can be a problem in XRF when X-ray penetration depth exceeds the thickness of the artefact, it is essentially the mass in general that is important in whole rock analyses.

Atmosphere

Air readily absorbs low energy X-rays, particularly for elements below titanium in the periodic table. Since argon makes up 1% of the composition of air and has an absorption edge below K and Ca, air also absorbs X-rays from those elements. It is common when analysing low Z elements to change the atmosphere by purging the chamber with helium (for liquids) or evacuating it entirely for solids. Lundblad et al. discuss in Chap. 4 and (2008) that all their analyses are conducted in a vacuum because of the dominance of the analysis of heterogeneous basalts non-destructively. It is necessary for low Z elements but is useful in their work for all elements of interest, even for those with $Z \approx 41$. Evacuating the analysis chamber is preferred when analysing all the low Z elements, since a vacuum does not absorb X-rays.

Purging is not recommended when analysing higher energy elements. Because the light element X-ray intensities are higher when the chamber is purged, there are fewer available counts for the heavy elements. When air is in the chamber, more current is required to achieve optimal count rates, and the net affect is improved sensitivity for the heavier elements. In this way the air functions as a neutral density detector filter that reduces light element intensities.

Count Time

The standard criteria for selecting count times are convenience and precision. Most analysts will use measurement times from 10 s to 10 min. Shorter count times 10–30 s are used more for qualitative scanning and sorting. The concentration range of the elements of interest is also important. Major elements in percent concentrations can be analysed in a minute or less, while minor elements at PPM concentrations may need to be analysed for 3–10 min or longer. The other and ultimately more important criterion is precision. Unfortunately measurement precision cannot be determined until after a calibration is complete, because only then is the calibration slope known. Most operators will use longer count times than necessary at first, in order to avoid having to repeat the calibration later.

Obsidian analysts in the U.S. who use EDXRF generally irradiate for 150–300 live seconds. However, as Giaque et al. found, increasing the counting time can increase precision, all other factors held equal (1993). One must evaluate the effort to achieve great precision over the accuracy needed to assign artifacts to source however (Shackley, 2002).

X-Ray Detection

Once a sample has been excited to fluorescence, a detector is used to convert X-rays into electronic signals which can be used to determine energy and intensity (number of X-rays) emitted from the sample. There are two types of detectors commonly used, the proportional counter used in WXRf and the semiconductor detector. The former is rarely used in archaeological applications.

The Si(Li) Detector

The Si(Li) semiconductor detector incorporates a silicon chip, which responds to X-rays by producing a charge at the detector output. This charge is converted into a voltage pulse which is then directed to pulse processing (Fig. 2.6). In the Si(Li) detector incident X-rays produce ionizations of the Si. The sensitive Si region is increased through the use of a process known as lithium drifting. Incident X-rays produce ionizations of Si in the sensitive regions of these detectors. The charge carriers are negative electrons and positive “holes”, which are drawn to opposite ends of the detector due to the voltage bias applied across the silicon chip. Total charge collected within the semiconductor detector is directly proportional to the energy of the incipient X-ray, and is converted to a corresponding voltage amplitude through the use of the preamplifier and amplifier (see Fig. 2.6). For the

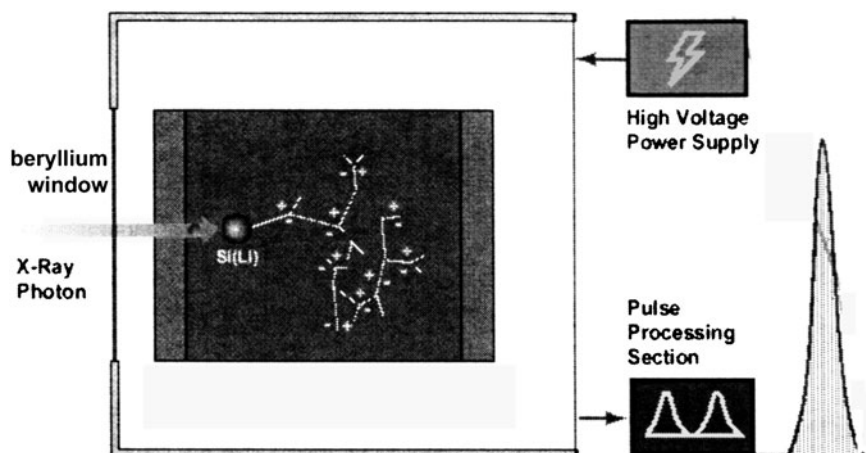


Fig. 2.6 Schematic representation of a Si(Li) detector in an EDXRF system

ionization to occur, the detector must be kept at very low temperatures and high vacuum, and it is sealed by a beryllium foil at the entry point.

Recently new germanium detectors and silicon drift detectors (SDD) without lithium are achieving better count rates and/or better resolution than Si(Li) detectors used most often in archaeological applications. These new X-ray detectors have yet to be applied in geoarchaeology, but will soon, perhaps solving some of the precision issues discussed above.

Pulse Processing

Charges produced in response to ionization in the detector are fed through a preamplifier and emerge from the detector output and need to be smoothed in the amplifier which gives them a pulse shape. Finally, these pulsed data are sent to the multi-channel analyzer (MCA), which converts the analogue pulses into channels. A channel is a memory location representing a small range of energies. As each pulse is digitized, it is stored in a channel corresponding to its amplitude (representing an X-ray energy level) and a counter for that channel is incremented by 1. The end result of these measurements is a collection of stored digital signals sorted by pulse height. These values are displayed graphically as a frequency distribution (histogram of energy vs. intensity) referred to as the *spectrum* (see Figs. 2.2 and 2.3), and further reduced through the calibration routine software into useable weight percent or parts per million data. At all stages in the pulse processing chain, proportionality between the detected X-ray energy, the analogue pulse amplitude, the digital signal value, and the corresponding channel number is strictly maintained.

Instrument Standards and Empirical Calibration

Students often ask, “How do you compare the results from one lab with another?” The answer is relatively simple. All laboratories, regardless of the type of instrument used, calibrate their instruments using the same international standards, mostly rock standards. These rock standards are supplied as powdered samples from mainly federal institutions from any number of countries, including the U.S. Geological Survey, the U.S. National Institute of Standards and Technology, and the Geological Surveys of Canada, France, Japan and South Africa (see Appendix). Additionally, during each analytical session, a selected standard is run with the unknown samples in order to determine whether the instrument is running within acceptable parameters, and just as important, so that other labs can evaluate the results compared to theirs.

For many years, the Berkeley lab has collaborated with those at the University of Missouri (Michael Glascock), the Geochemical Research Laboratory (Richard Hughes), and the Northwest Research Obsidian Studies Laboratory (Craig Skinner), and in some cases we may have to evaluate the data from one or another of the labs, and I have always found the data so similar to source data from my lab, that I can readily determine the source. The differences are within a few percent, often only 1%. Of course, both Hughes and Skinner use the same software and instrument, but even the NAA and XRF data of Mike Glascock at Missouri are within a percent or two for most elements, except for those elements that XRF does not measure well or vice-versa (see Chap. 8).

The instrument settings for the ThermoScientific Quant’X at Berkeley are in the Appendix, but just how does an XRF analyst set up a method to analyse volcanic rocks? The minor details between these different instruments and laboratories are slightly different, but the trajectory is essentially the same.

The EDXRF Quantitative Method Trajectory

As with any good research project, the research plan must be formulated first:

- What is the sample type – pressed powder, fused disk, whole rock?
- What are the elements of interest – major oxides, trace elements, rare earths?
- What level of precision is acceptable?
- What level of accuracy is necessary to assign to source?
- Conditions to be used- measurement time, voltage, amperage?
- What standards are available or necessary?

After the outline of research, the first step in EDXRF is to acquire the elements and generate elemental peak profiles. This is necessary for the peak-fitting algorithms that correct for overlap and background. Pure elements purchased from a number of suppliers in powder form are acquired by a software utility and incorporated into the method file. For lighter elements, and those that will measure L lines, the same voltage and filter settings should be the same.

The next step is to select the conditions and elements of interest. Most instrument software restricts the selection to only those that can be optimally acquired given the conditions selected. This eliminates many problems of interpretation.

The next step is to create a standards library. Standards libraries are separate files that contain standards used to calibrate the method. Separate standards libraries may be used for various methods or conditions. At Berkeley, we have separate standards libraries for the oxides using fused disk standards and for trace elements using pressed powder standards. This is a typical XRF strategy, but see Lundblad et al. (2008) for a non-destructive analytical strategy for basalt. An important consideration when selecting standards is that they should exhibit the entire range of variation expected from the rocks to be analysed. For obsidian (rhyolite), this would include (for strontium for example) a range between zero and around 500–600 ppm. It is rare for a rhyolite to be much above 200 ppm. In the Berkeley case, we also analyse basalt, dacite, and other rocks as well as ceramics, and so include standards from all the major volcanic rock groups, and the ceramic standard SARM-69 from South African Neolithic pottery (see Appendix).

After importing the standards for a given method, the instrument is calibrated using the expected (given) elemental concentrations (let us say ppm) from the standards vs. the calculated elemental concentrations (ppm). This is called *empirical calibration* as opposed to a fundamental parameters calibration. In this case a linear algorithm is used for calibration and all the standards are analysed as unknowns and the elemental data from each standard is plotted relative to a best fit regression line (Fig. 2.7). For the oxide fundamental parameters analysis, a quadratic regression may be used. Fundamental parameters calibrations use a variety of calculus functions to predict the expected values, although some are also based on a linear algorithm.

After the instrument completes the calibration routine, a table and regression scattergram is produced. The fit to the line can be improved by elimination of data from any standard until a best fit is achieved (Fig. 2.7). This could require a number of calibrations. Figure 2.7 exhibits the calculated vs. given concentrations for Sr in the Quant'X system. In this case, none of the standards have been removed. The 17 standards included in the analysis vary from near zero ppm Sr for JR-1 (40 ppm) and JR-2 (39 ppm), Japan Geological Survey rhyolite standards to nearly 1,300 ppm for BR-N, a Geological Survey of France basalt standard. The good fit of the standards on the regression line indicates that the analysed concentrations were at or near the given concentrations recommended by the various institutions or the Geostandards Newsletter (Govindaraju, 1994). The recommended data for each element of each standard is an arithmetic mean of data submitted by laboratories worldwide for those particular elements and standards.

The calculated values for various elements in the Geostandards Newsletter are used by most laboratories around the world, so each lab expects, for example, that RGM-1 USGS obsidian standard should yield an elemental concentration at about 108 ppm. Again, this shows that each instrument is properly calibrated and allows scientists from other institutions to evaluate interlab bias.

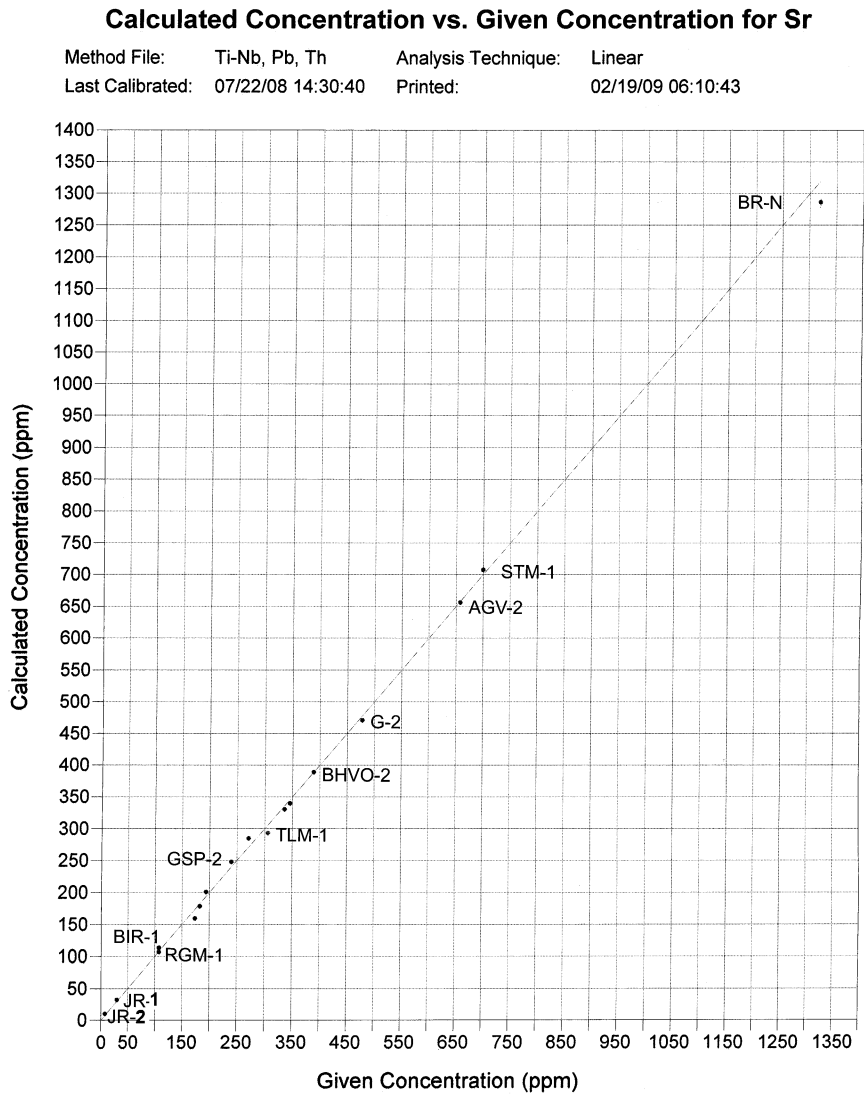


Fig. 2.7 Given (x-axis) vs. calculated (y-axis) calibration curve for Sr on the ThermoScientific Quant'X using 17 international standards (see Appendix for list of standards). Only selected standards noted. All are present

Qualitative Analysis

There is little archaeological literature covering XRF qualitative analyses, but it is a routine frequently used to determine the relative composition of a substance. Qualitative analysis is the detection of elements without applying rigorous

quantification methods. We frequently use it to determine whether an element or set of elements are present. As mentioned above, a qualitative analysis can aid in determining which elements best discriminate a given obsidian source or sources within a geographic region. It is impossible to come up with a single acquisition condition that excites every element well with low background in every region of interest. To overcome this problem a qualitative analytical procedure will consist of three or more different sets of acquisition conditions. Three basic acquisition conditions cover the same low, medium, and high energy ranges discussed previously.

Figure 2.8 shows a qualitative analysis of the USGS RGM-1 standard. Compare with Figs. 2.2 and 2.3, quantitative analyses of the same standard, actually the same sample. This medium count qualitative analysis between about 1 and 20.48 keV does indicate the elemental composition of this obsidian. It does not tell you the quantity of each element but does show the elements in relative proportion given background. Note that the bremsstrahlung (continuous) background is readily observable under the labelled Rb–Zr elemental peaks (the hump-shaped region at ~10–19 keV).

Qualitative analyses like this are frequently used in environmental studies to determine the presence of elements of interest, such as lead in paints, mercury in water, and other contaminants. This is an application where PXRF is particularly

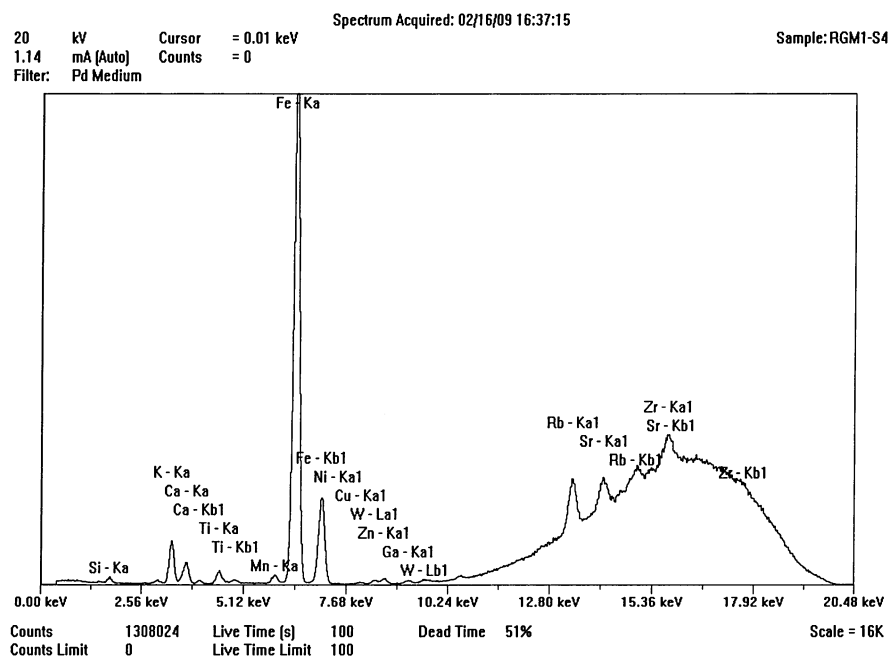


Fig. 2.8 A spectrum from a qualitative scan of RGM-1, showing the continuous radiation (bremsstrahlung) scatter apparent under the Rb–Zr peaks

well adapted. We use it frequently in the XRF lab at Berkeley just to determine the presence of elements in various solids, from unknown rocks to the relative proportions of elements on gold rings, or to determine whether a piece of jewellery is actually made of the metal the seller thinks it is made of.

Wavelength vs. EDXRF

Most of the discussions above have focused on EDXRF, and the descriptions of the instruments have been directed toward EDXRF. Wavelength XRF was the first to be used in archaeological analyses simply because it was the first invented, but by the 1970s EDXRF began to replace some of the WXRf systems in geological departments until the ICP-MS “revolution” in the 1990s. Today, WXRf is still the XRF system preferred in many geology institutions when an order of precision greater than EDXRF is required, particularly for light elements. Figures 2.9 and 2.10 show schematic renderings of both systems.

As in energy-dispersive systems, the WXRf X-ray source is quite similar. An anode of an appropriate element is paired with a target of an appropriate element for the elements of interest. However, in many modern WXRf systems, a number of tubes, and/or multiple targets are used in order to maximize the instrumental precision for $Z = 11\text{--}92$. In wavelength dispersive spectrometers, fluorescence

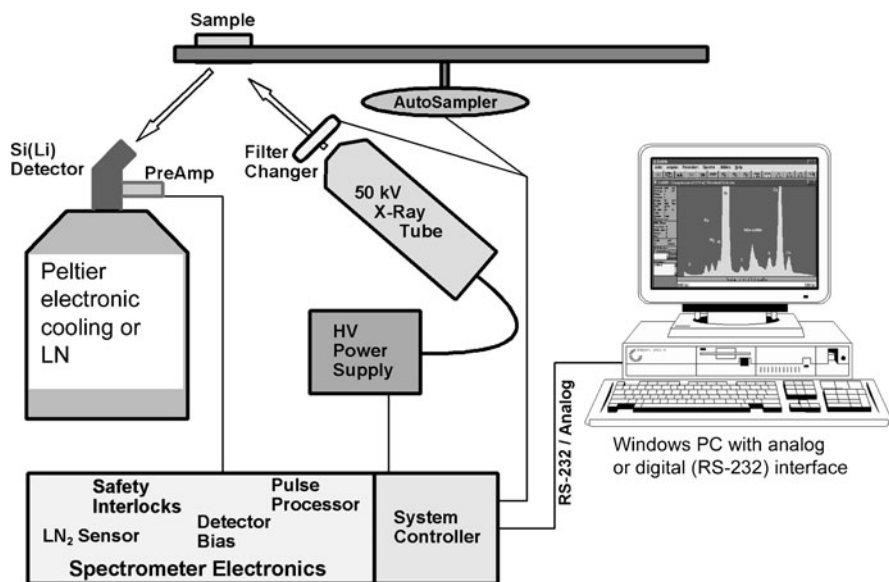


Fig. 2.9 Schematic drawing of a typical EDXRF instrument. Cooling can be either electronic Peltier or liquid nitrogen (LN)

X-ray photons are separated by *diffraction* on a single crystal before being detected. Although wavelength dispersive spectrometers are occasionally used to scan a wide range of wavelengths, producing a spectrum plot as in EDXRF, they are usually set up to make measurements only at the wavelength of the emission lines of the elements of interest, one element at a time. Collimation becomes even more important in WXRf to focus the incident X-rays toward the analysing crystal at the appropriated Bragg angle (Fig. 2.10). Importantly, unlike EDXRF, each element is selected by appropriate crystals individually according to Bragg's Law:

$$\begin{aligned} n \lambda &= 2d \cdot \sin\theta \\ \text{or alternatively} \\ \lambda &= (2d/n)\sin\theta \end{aligned} \quad (2.2)$$

where

- n is an integer determined by the order given
- λ is the wavelength of X-rays, and moving electrons, protons and neutrons
- d is the spacing between the planes in the atomic lattice, and
- θ is the angle between the incident ray and the scattering planes (see Fig. 2.9)

While the “early” WXRf instruments like the old Philips instruments at Berkeley and Arizona State University required manual selection of the analysing crystals with a manual goniometer, modern systems like the Philips 2400 WXRf at Berkeley are completely automated. After selecting the elements of interest and calibrating the instrument, the software selects the appropriate target(s) and crystal(s) based on that selection (see Jenkins, 1999 for more detail).

While instrumental precision in EDXRF systems has increased greatly in the last decade, WXRf instruments, simply because they are not separating all the seemingly chaotic energy entering the detector into individual channels and then into elemental data through preamplification, but selecting each element individually,

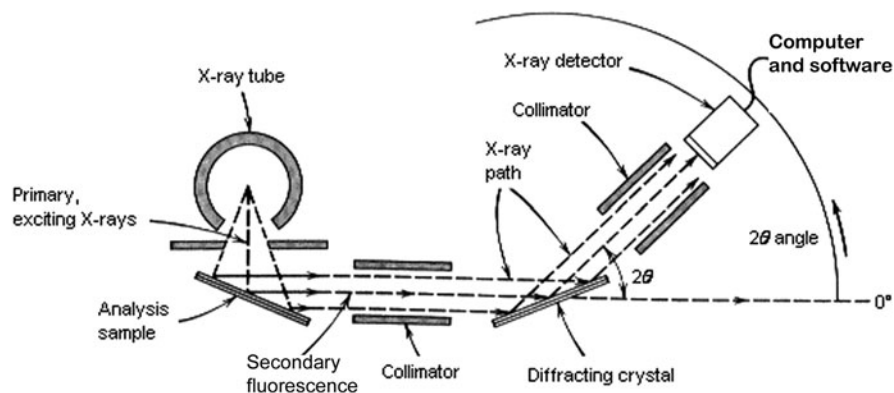


Fig. 2.10 Schematic drawing of a typical WXRf system. Only a single tube/target is shown here

Table 2.3 Detection limits (% for oxides, ppm for elements) for selected major and trace elements in whole rock EDXRF vs. WXRf (from Jenkins, 1999, 119)

| Element | EDXRF | WXRf |
|-------------------|-------|-------|
| Na ₂ O | 0.81 | 0.16 |
| Ti | 0.008 | 0.006 |
| Mn | 0.002 | 0.014 |
| Rb | 3.0 | 0.6 |
| Sr | 2.8 | 0.4 |
| Y | 3.8 | 0.4 |
| Zr | 2.8 | 1.1 |
| Nb | 2.8 | 1.3 |

are much more precise particularly in the lighter elements or calculated oxides such as Na. Table 2.3 shows a comparison of instrumental precision between EDXRF and WXRf for various elements. Again, as I have said repeatedly, the analyst and/or archaeologist must decide which level of precision and accuracy is desired or necessary (Shackley, 2002).

Non-Destructive WXRf Analyses

De Francesco et al. in Chap. 5 discuss a non-destructive qualitative analysis of archaeological obsidian with WXRf comparing favourably to destructive quantitative analyses. One of the major reasons that qualitative analyses have been favoured for WXRf work is that the Bragg angle assumes that the sample surface is absolutely flat or parallel to the crystal. Unfortunately, artifacts are not flat. So, by ratioing the elements against each other, the errors in the Bragg become “balanced” as I discussed above. However, most modern WXRf software will allow an analyst to perform a calibration based on ratioing to the Compton scatter just as in most EDXRF analyses. Tim Teague of the Department of Earth and Planetary Sciences at Berkeley and I have been doing this on the Philips PW2400 for a decade with precision equal to any EDXRF analysis, indeed without some of the issues with the heavier elements such as Ba in EDXRF (Shackley 1998a, 2005). The Philips *SuperQ* software has this utility, but few use it. One advantage of this is that a large number of elements can be acquired more rapidly than with the EDXRF systems that generally require a different set of conditions for each set of elements and instrument settings. The major limitation with most of the WXRf systems, as mentioned by De Francesco et al. in Chap. 5, is that the sample holders are of a limited size, 41 mm in the Philips PW 2400 case at Berkeley. In many EDXRF systems, the chamber is quite large and can be made even larger, as in the Hawaii-Hilo QuanX (Lundblad et al., 2008; Chap. 4). Additionally, the WXRf systems must run under vacuum. Air path analyses are not readily possible. So, while WXRf instruments can provide greater instrumental precision, there are limiting factors that can make EDXRF a better choice.

Analytical Instrument Settings and Providing Data

As part of the goal of this volume, we are trying to make XRF as understandable and transparent as we can to the curious archaeological community. We are also, of course, responsible for providing the data from our research to the public, which provides the bulk of our funding. For a number of years Mike Glascock (the author of Chap. 8) and I have been attempting to put all our obsidian source data on the web for the public, our supporting public. The elemental, geographic, and geological data from all known obsidian sources in the North American Southwest are on the web at: <http://swxrfllab.net/swobsrsrcs.htm> and every effort is made to keep it up to date.

Immediately after a newly discovered source is published in print, I put the data online. Our job in the XRF community is to publish that data as soon as possible. Results are published in journals like *American and Latin American Antiquity*, *Antiquity*, *Archaeometry*, *Geoarchaeology*, *Journal of Archaeological Science*, and many other regional journals around the world.

Just as important is the publishing of the instrumental settings and analytical strategies used. This is necessary to evaluate one another's work, and for the archaeologist to understand what he or she is doing and whether the analytical strategy is sensible. I hope that after reading this chapter, the analytical trajectory and instrument settings that I give to you (the archaeologist) in each full report and in the Appendix here will be more comprehensible.

References

- Asaro, F. and D. Adan-Bayewitz, (2007), The history of the Lawrence Berkeley National Laboratory Instrumental Neutron Activation Analysis Programme for Archaeological and Geological Materials. *Archaeometry* 49, 201–214.
- Bertin, E., (1978), *Introduction to X-ray spectrometric analysis*. New York: Plenum.
- Bouey, P., (1991), Recognizing the limits of archaeological applications of non-destructive energy-dispersive X-ray fluorescence analysis of obsidians. *Materials Research Society Proceedings* 185, 309–320.
- Buras, B., Olsen, J.S., Andersen, A.L., Gerward, L., and Selsmark, B., (1974), Evidence of escape peaks caused by a Si(Li) detector in energy-dispersive diffraction spectra. *Journal of Applied Crystallography* 7:296–297.
- Cann, J.R., (1983), Petrology of obsidian artifacts. In Kempe D.R.C., and Harvey A.P., (Eds.), *The Petrology of Archaeological Artefacts*, (pp. 227–255). Oxford: Clarendon.
- Cann, J.R., and Renfrew, A.C., (1964), The characterization of obsidian and its application to the Mediterranean region. *Proceedings of the Prehistoric Society* 30, 111–133.
- Cesareo, R., Ridolfi, S., Marabelli, M., Castellano, A., Buccolieri, G., Donativi, M., Gigante, G.E., Brunetti, A., and Medina, M.A.R., (2008), Portable systems for energy-dispersive X-ray fluorescence analysis of works of art. In Potts, P.J., and West, M. (Eds.), *Portable X-ray fluorescence spectrometry: capabilities for in situ analysis*, (pp. 206–246). Cambridge: The Royal Society of Chemistry.

- Craig, N., Speakman, R.J., Popelka-Filcoff, R.S., Glascock, M.D., Robertson, J.D., Shackley, M.S., Aldenderfer, M.S., (2007), Comparison of XRF and PXRF for analysis of archaeological obsidian from southern Perú. *Journal of Archaeological Science* 34 (12), 2012–2024.
- Davis, M. K. 1994 Bremsstrahlung ratio technique applied to the non-destructive energy-dispersive X-ray fluorescence analysis of obsidian. *International association for obsidian studies bulletin* 11.
- Davis, M.K., Jackson, T.L., Shackley, M.S., Teague, T., and Hampel, J., (1998), Factors affecting the energy-dispersive X-ray fluorescence (EDXRF) analysis of archaeological obsidian. In M.S. Shackley (Ed.), *Archaeological obsidian studies: method and theory*, (pp. 159–180). Advances in archaeological and museum studies 3. New York: Springer/Plenum Press.
- Dillian, C.D., (2002), *More than toolstone: differential utilization of glass mountain obsidian*. Ph. D. dissertation, Department of Anthropology, University of California, Berkeley.
- Eerkens, J.W., Ferguson, J.R., Glascock, M.D., Skinner, C.E., and Waechter, S.A., (2007), Reduction strategies and geochemical characterization of lithic assemblages: a comparison of three case studies from Western North America. *American Antiquity*, 72, 585–597.
- Franzini, M., L. L. and Saitta M., (1976), Determination of the X-ray fluorescence mass absorption coefficient by measurement of the intensity of Ag K α compton scattered radiation. *X-ray Spectrometry* 5, 84–87.
- Giaque, R. D., Asaro, F., and Stross, F. H., (1993), High precision non-destructive X-ray fluorescence method applicable to establishing the provenance of obsidian artifacts. *X-ray Spectrometry*, 22, 44–53.
- Glascock, M.D., Braswell, G.E., and Cobean, R.H., (1998), A systematic approach to obsidian source characterization. In M.S. Shackley (Ed.), *Archaeological obsidian studies: method and theory*, (pp. 15–66). Advances in archaeological and museum studies 3. New York: Springer/Plenum Press.
- Goldberg, P., (2008), Raising the bar: making geological and archaeological data more meaningful for understanding the archaeological record. In Sullivan, A., Ed., *Archaeological concepts for the study of the cultural past*, (pp. 24–39). Salt Lake City: University of Utah Press.
- Govindaraju, K., (1994), 1994 compilation of working values and sample description for 383 geostandards. *Geostandards Newsletter* 18 (special issue).
- Hall, E.T., (1960), X-ray fluorescent analysis applied to archaeology. *Archaeometry* 3, 29–37.
- Hampel, J.H., (1984), Technical considerations in X-ray fluorescence analysis of obsidian. In Hughes, R. E. (Ed.), *Obsidian Studies in the Great Basin*, (pp. 21–25). Berkeley: Contributions of the University of California Archaeological Research Facility 45.
- Huckell, B.B., Holliday, V.T., Hamilton, M., Sinkovec, C., Merriman, C., Shackley, M.S., and R.H. Weber, The Mockingbird Gap Clovis Site: 2007 investigations. *Current Research in the Pleistocene* 25, 95–97.
- Hughes, R.E., (1983), *Exploring diachronic variability in obsidian procurement patterns in northeast California and southcentral Oregon: geochemical characterization of obsidian-sources and projectile points by energy-dispersive X-ray fluorescence*. Ph.D. dissertation, Department of Anthropology, University of California, Davis.
- Hughes, R.E., Ed., (1984), *Obsidian Studies in the Great Basin*. Berkeley: Contributions of the University of California Archaeological Research Facility 45.
- Hughes, R.E., (2010) *Determining the geologic provenance of tiny obsidian flakes in archaeology using nondestructive EDXRF*. *American Laboratory* 42, 27–31.
- Hull, Kathleen L., (2002) *Culture contact in context: a multiscalar view of catastrophic depopulation and culture change in Yosemite Valley*. Ph.D. dissertation, Department of Anthropology, University of California, Berkeley, CA.
- Ivanenko, V.V., Kustov, V.N., and Matelev, A.Yu., (2003), Patterns of inter-elemental effects in EDXRF and a new correction method. *X-ray spectrometry* 32, 52–56.
- Jack, R.N., (1971), The source of obsidian artifacts in northern Arizona. *Plateau* 43, 103–114.

- Jack, R.N., (1976), Prehistoric obsidian in California: geochemical aspects. In Taylor, R.E., Ed., *Advances in obsidian glass studies: archaeological and geochemical perspectives*, (pp. 183–217). Park Ridge, NJ: Noyes Press.
- Jack, R.N., and Carmichael, I.S.E., (1969), The chemical fingerprinting of acid volcanic rocks. *California division of mines and geology special report* 100, 17–32.
- Jack, R.N. and Heizer, R.F., (1968) “Finger-Printing” of some Mesoamerican obsidian artifacts. Berkeley: Contributions of the University of California Archaeological Research Facility 5, 81–100.
- Jackson, T.L., (1974), *The economics of obsidian in central California prehistory: applications of X-ray fluorescence spectrography in archaeology*. Master’s thesis, Department of Anthropology, San Francisco State University, San Francisco.
- Jackson, T.L., (1986), *Late prehistoric obsidian exchange in central California*. Ph.D. dissertation, Department of Anthropology, Stanford University.
- Jackson, T.L. and Hampel, J.H. (1992). Size Effects in the Energy-Dispersive X-ray Fluorescence (EDXRF) Analysis of Archaeological Obsidian Artifacts. Poster presented at the 28th International Symposium on Archaeometry, Los Angeles.
- Jenkins, R., (1999), *X-ray fluorescence spectrometry: second edition*. New York: Wiley-Interscience.
- Jenkins, R., Gould, R.W., and Gedcke, D., (1981), *Quantitative X-ray spectrometry*. New York: Marcel Dekker.
- Joyce, R.A., Shackley, M.S., Sheptak, R. and McCandless, K., (2004), Resultados preliminares de una investigación con EDXRF de obsidiana de Puerto Escondido. In *memoria, vii seminario de antropología de Honduras “Dr. George Hasemann”*, (pp. 115–130). Instituto Hondureño de Antropología e Historia, Honduras.
- Kahn, J.G., (2005) *Household and community organization in the late prehistoric Society Island Chiefdoms (French Polynesia)*. Ph.D. dissertation, Department of Anthropology, University of California, Berkeley.
- Killick, D., (2008), Archaeological science in the USA and in Britain. In Sullivan, A., Ed., *Archaeological concepts for the study of the cultural past*, (pp. 40–64). Salt Lake City: University of Utah Press.
- Lachance, G.R., and Claisse, F., (1994), *Quantitative X-ray fluorescence analysis*. New York: Wiley-Interscience.
- Lundblad, S. P., Mills, P. R., & Hon, K. (2008). Analysing archaeological basalt using non-destructive energy-dispersive X-ray fluorescence (EDXRF): Effects of post-depositional chemical weathering and sample size on analytical precision. *Archaeometry*, 50, 1–11.
- Martynec, R., Davis, R., and Shackley, M.S., (2010), The Los Sitios del Agua Obsidian source (formerly AZ unknown a) and recent archaeological investigations along the Rio Sonoyta, northern Sonora. *Kiva*, in press.
- McCarthy, J.J., and Schamber, F.H. (1981) Least-squares fit with digital filter: a status report. In Heinrich, K.F.J., Newbury, D.E., Myklebust, R.L., and Fiori, E. (Eds.), *Energy Dispersive X-ray Spectrometry*, (pp. 273–296). Washington, D.C.: National Bureau of Standards Special Publication 604.
- Moseley, H.G.J., (1913/1914), High frequency spectra of the elements. *The philosophers magazine*, 26, 1024–1034, and 27, 703–713.
- Nazaroff, A., and Shackley, M.S., (2009), Testing the size dimension limitation of portable XRF instrumentation for obsidian provenance. Poster presentation, Geological Society of America Annual Meeting, Portland, OR.
- Negash, A. and Shackley, M.S., (2006), Geochemical provenance of obsidian artefacts from the MSA site of Porc Epic, Ethiopia. *Archaeometry* 48, 1–12.
- Negash, A., Shackley, M.S. and Alene, M., (2006) Source provenance of obsidian artifacts from the Early Stone Age (ESA) site of Melka Konture, Ethiopia. *Journal of Archaeological Science* 33, 1647–1650.

- Pessanha, S., Guilherme, A., and Carvalho, M.L., (2009), Comparison of matrix effects on portable and stationary XRF spectrometers for cultural heritage samples. *Applied Physics A* 97, 497–505.
- Phillips, S.C., and Speakman, R.J., (2009), Initial source evaluation of archaeological obsidian from the Kuril Islands of the Russian Far East using portable XRF. *Journal of Archaeological Science* 36, 1256–1263.
- Potts, P.J. and West, M., Eds., (2008), *Portable X-ray fluorescence spectrometry: capabilities for in situ analysis*. Cambridge: The Royal Society of Chemistry.
- Rindby, A., (1989), Software for energy-dispersive X-ray fluorescence. *X-ray spectrometry*, 18, 113–118.
- Röntgen, W.K., (1898), On a new kind of rays: second communication. *Annals of Physical Chemistry*, 64, 1–11.
- Schamber, F.H., (1977) A modification of the linear least-squares fitting method which provides continuum suppression. In Dzubay, T.G. (Ed.), *X-ray Fluorescence Analysis of Environmental Samples*, (pp. 241–257). Ann Arbor: Ann Arbor Science.
- Shackley, M. S., (1988), Sources of archaeological obsidian in the Southwest: an archaeological, petrological, and geochemical study. *American Antiquity* 53, 752–772.
- Shackley, M.S., (1990). *Early hunter-gatherer procurement ranges in the Southwest: evidence from obsidian geochemistry and lithic technology*. Ph.D. dissertation. Tempe: Arizona State University.
- Shackley, M.S., (1991) Tank Mountains obsidian: a newly discovered archaeological obsidian source in east-central Yuma County, Arizona. *Kiva* 57, 17–25.
- Shackley, M.S., (1992). The Upper Gila River gravels as an archaeological obsidian source region: implications for models of exchange and interaction. *Geoarchaeology* 4, 315–326.
- Shackley, M.S., (1995), Sources of archaeological obsidian in the greater American Southwest: an update and quantitative analysis. *American Antiquity* 60, 531–551.
- Shackley, M.S., (1998a), Geochemical differentiation and prehistoric procurement of obsidian in the Mount Taylor Volcanic Field, Northwest New Mexico. *Journal of Archaeological Science* 25, 1073–1082
- Shackley, M.S., (1998b) Intrasource chemical variability and secondary depositional processes in sources of archaeological obsidian: lessons from the American Southwest. In Shackley, M.S. (Ed.), *Archaeological obsidian studies: method and theory* (pp. 83–102). Advances in archaeological and museum science 3. New York: Springer/Plenum.
- Shackley, M.S., Ed., (1998c), *Archaeological obsidian studies: method and theory*. Advances in Archaeological and Museum Science 3, New York: Springer/Plenum Publishing Corporation.
- Shackley, M.S., (2002) Precision versus Accuracy in the XRF analysis of archaeological obsidian: some lessons for archaeometry and archaeology. In Jerem, E., and Biro, K.T., Eds. *Proceedings of the 31st Symposium on Archaeometry, Budapest, Hungary*, (pp. 805–810). Oxford: British Archaeological Reports International Series 1043 (II).
- Shackley, M.S., (2005), *Obsidian: geology and archaeology in the North American Southwest*. Tucson: University of Arizona Press.
- Shackley, M.S., (2010), Is there reliability and validity in portable X-ray fluorescence spectrometry (PXRF)? SAA Archaeological Record (in press).
- Shackley, M.S. and Dillian, C., (2002), Thermal and environmental effects on obsidian geochemistry: experimental and archaeological evidence. In Loyd, J.M, Origer, T. M. and Fredrickson, D.A. (Eds.), *The effects of fire and heat on obsidian*, (pp. 117–134). Sacramento: Cultural resources publication, anthropology-fire history, U.S. Bureau of Land Management.
- Shackley, M. S. and Hampel, J., (1992), Surface effects in the energy dispersive X-ray fluorescence (EDXRF) analysis of archaeological obsidian. Poster presented at the 28th International Symposium on Archaeometry, Los Angeles.
- Silliman, S., (2000), *Colonial worlds, indigenous practices: the archaeology of labor on a 19th century California rancho*. Ph.D. dissertation, Department of Anthropology, University of California, Berkeley.

- Speakman, R.J. and Neff, H., Eds., (2005), *Laser ablation ICP-MS in archaeological research*. Albuquerque: University of New Mexico Press
- Weisler, M. I., (1993), *Long-distance interaction in Prehistoric Polynesia: three case studies*. Ph. D. dissertation, Department of Anthropology, University of California, Berkeley.
- Weisler, M.I., and Woodhead, J.D., (1995), Basalt Pb isotope analysis and the prehistoric settlement of Polynesia. *Proceedings of the National Academy of Science*, 92, 1881–1885
- Williams-Thorpe, O., (2008), The application of portable X-ray fluorescence analysis to archaeological lithic provenancing. In Potts, P.J., and West, M. (Eds.), *Portable X-ray fluorescence spectrometry: capabilities for in situ analysis*, (pp. 174–205). Cambridge: The Royal Society of Chemistry.

X-Ray Fluorescence Spectrometry (XRF) in
Geoarchaeology

Shackley, M.S. (Ed.)

2011, XIV, 231 p. 32 illus., 11 illus. in color., Hardcover

ISBN: 978-1-4419-6885-2